

# UC Berkeley

## UC Berkeley Previously Published Works

### Title

Uncoupling heart cell specification and migration in the simple chordate *Ciona intestinalis*

### Permalink

<https://escholarship.org/uc/item/1j21k7ww>

### Journal

Development, 132(21)

### ISSN

0950-1991

### Authors

Davidson, Brad  
Shi, Weiyang  
Levine, Michael

### Publication Date

2005-11-01

Peer reviewed

# Uncoupling heart cell specification and migration in the simple chordate *Ciona intestinalis*

Brad Davidson\*, Weiyang Shi and Michael Levine

Department of Molecular and Cellular Biology, Division of Genetics and Development, University of California, Berkeley, CA 94720, USA

\*Author for correspondence (e-mail: bandl@berkeley.edu)

Accepted 22 August 2005

Development 132, 4811–4818  
Published by The Company of Biologists 2005  
doi:10.1242/dev.02051

## Summary

The bHLH transcription factor *Mesp* has an essential but ambiguous role in early chordate heart development. Here, we employ the genetic and morphological simplicity of the basal chordate *Ciona intestinalis* to elucidate *Mesp* regulation and function. Characterization of a minimal cardiac enhancer for the *Ciona Mesp* gene demonstrated direct activation by the T-box transcription factor *Tbx6c*. The *Mesp* enhancer was fused to GFP, permitting high-

resolution visualization of heart cells as they migrate and divide. The enhancer was also used to drive targeted expression of an activator form of *Mesp*, which induces heart formation without migration. We discuss the implications of *Tbx6-Mesp* interactions for the evolution of cardiac mesoderm in invertebrates and vertebrates.

Key words: Cardiac specification, Migration, Chordate, *Mesp*

## Introduction

The *Ciona* heart field can be traced to a single pair of cells in 110-cell embryos, the B7.5 blastomeres (Davidson and Levine, 2003; Hirano and Nishida, 1997). *Mesp* is the only regulatory gene expressed exclusively in these cells (Imai et al., 2004; Satou et al., 2004). During gastrulation, the B7.5 blastomeres divide into two distinct lineages. The rostral daughters (trunk ventral cells or TVCs) migrate to form the heart, while the caudal daughters remain in the tail and differentiate into anterior tail muscle cells (Fig. 1A). Homology to vertebrate heart cells becomes evident after neurulation, when TVCs express orthologs of the core cardiac regulatory genes *Nkx2.5*, *Hand* (Davidson and Levine, 2003; Satou et al., 2004) and *Gata4* (B.D., unpublished). The TVCs then migrate anteriorly and ventrally to fuse along the ventral midline in a manner reminiscent of vertebrate heart cell migration (Davidson and Levine, 2003). After metamorphosis, the *Ciona* heart rudiment differentiates into a contractile linear tube, which expresses orthologs of vertebrate heart structural genes including a cardiac-specific splice variant of *Troponin I* (MacLean et al., 1997).

*Mesp* is expressed in the emerging heart field of mouse embryos prior to expression of the core cardiac regulatory genes (Saga et al., 2000). There are two *Mesp* paralogs, and chimeric cells lacking both (*Mesp1* and *Mesp2*) display cell autonomous defects in heart formation (Kitajima et al., 2000). *Ciona* contains a single *Mesp* gene. Morpholino-based suppression of *Mesp* function in *Ciona savignyi* causes a block in heart cell migration and specification, leading to the formation of supernumerary tail muscle cells (Satou et al., 2004). Despite the central importance of *Mesp* function in early chordate heart development, the factors that direct *Mesp* expression in the emerging heart field have not been defined

(Haraguchi et al., 2001). Furthermore, it remains to be determined whether *Mesp* functions primarily as a migration factor, as inferred from vertebrate analyses, or as a specification factor, as proposed in the *Ciona* study.

Here, we present evidence that *Ciona Mesp* is directly activated by the T-box transcription factor *Tbx6c*. There are three *Tbx6* paralogs in *Ciona*, *Tbx6a*, *Tbx6b* and *Tbx6c*. *Tbx6b* and *Tbx6c* are activated by the maternal muscle determinant *Macho 1*, and initiate muscle gene expression (Yagi et al., 2005). While *Tbx6b* has a predominant role in muscle specification, *Tbx6c* independently regulates gene expression in the anterior tail muscle lineage (Yagi et al., 2005).

The *Mesp* enhancer was used to selectively express an activator form of *Mesp* in the early heart field. Heart cell migration is inhibited, but beating heart tissue nonetheless differentiates at an ectopic location in the anterior tail. These results demonstrate that heart specification and migration can be uncoupled, and implicate *Mesp* as a crucial cardiac determinant.

## Materials and methods

### Ascidians: collection, handling and experimental techniques

*Ciona* adults were collected from Half Moon Bay, Oyster Point and San Diego (M-Rep, CA). No significant experimental discrepancies were observed among animals from different sources. Rearing, fertilization, dechoriation, in situ hybridization, electroporation and *lacZ* staining were conducted as described previously (Corbo et al., 1997). For double in situ hybridization, two techniques were used (the second protocol is a modified version of the TSA Plus Fluorescence Systems protocol, Perkin Elmer, USA). (1) *lacZ* was stained with Fast Red (Davidson and Levine, 2003) using a fluorescein-labeled probe, while *Tbx6c* was hybridized to a digoxigenin-labeled probe and

stained using AP/NBT/BCIP as described previously (Corbo et al., 1997). (2) *Tbx6c* or *Tbx6b* were stained with Fast Red using a DIG-labelled probe, the first antibody was then stripped by incubation for 10 minutes in 100 mM glycine-HCl (pH 2.2), 0.1% Tween-20 and then taken through four short rinses in PBT. The second antibody (anti-FITC-POD, Roche, USA) was subsequently applied at a 1:1500 dilution overnight at 4°C. Embryos were then quenched for 20 minutes in 0.3-3% hydrogen peroxide (in PBT), rinsed twice in PBT and then rinsed three times for 5 minutes in TNT buffer [0.1 M TRIS-HCl (pH 7.5), 0.15 M NaCl, 0.05% Tween-20]. Finally, the embryos were incubated in 300 µl freshly diluted (1:50) 1× Plus Fluorescein Tyramide Stock Solution for 15 minutes and mounted in Prolong Gold antifade reagent (Invitrogen, USA).

### Construction of transgenic DNAs

Genomic DNA was isolated from the pooled sperm of 3-4 adults, using the PureGene DNA Isolation kit (Gentra Systems), and used as a template for PCR-based isolation of the required genomic fragments. These fragments were then cloned into either the pCES vector (Harafuji et al., 2002) or modified versions of this vector, as described below.

### Mesp reporter constructs

The 5' flanking DNAs from *Ci-Mesp* and *Cs-Mesp* were initially isolated using the following primers [numbers indicate the base-pair (bp) distance 5' of the EST predicted transcript]:

*Ci-Mesp*f1916, gcgcTCTAGACGGTTCAACGTGACGTCCCAT-GC;

*Ci-Mesp*Natb, aaaGCGGCCCGCCATAATACAAGTTTCAAATC-AACCTG;

*Cs-Mesp*f1123, gcgcTCTAGATCTGAATGAGCAG; and

*Cs-Mesp*Natb, aaaGCGGCCCGCCATGAATACGTTTCCAGG.

The use of lowercase letters indicates padding on the primer that is not incorporated into the construct.

These fragments were fused in-frame with *lacZ* in the pCES vector using the PCR-generated *Xba*I and *Not*I sites, replacing the *Ci-forkhead* minimal promoter. These constructs were then used as templates for further 5' deletions using the appropriate forward primers. *Mesp* reporter constructs containing ~200 bp or less 5' DNA began to drive ectopic expression of *lacZ* in the tail muscles and sometimes in the notochord. However, it was determined that this ectopic expression was due to a vector artefact that was eliminated by removing an ~320 bp fragment of the vector in between the *Xba*I site and an *Eco*O1091 site upstream of the polylinker. In all subsequent constructs this area of the vector was removed. Single nucleotide mutations were generated by PCR amplification using primers with appropriately altered sequences. *Mesp*-GFP was constructed by replacing the *lacZ*-coding region from the *Mesp*1916-*lacZ* construct with the enhanced-GFP (eGFP)-coding region.

### Recombinant Mesp, MyoD constructs

The *Mesp* and *MyoD* bHLH DNA-binding domains were amplified from the *Mesp* EST clone (CiGC13m15) or the *MyoD* [*Ci-MDF* (Meedel et al., 1997)] EST clone (GC42d13), respectively, which were obtained from the *Ciona intestinalis* Gene Collection Release1 (Satou et al., 2002), using the following primers:

*Mesp*HLHf, aaaGCTAGCCAAGCGACAAACCGCTAGTGAAG-GAGAACG;

*Mesp*HLHb, aaaACTAGTGTTCGACGACGTTTTTCTTCTTG;

*MyoD*HLHf, aaaGCTAGCGCAGGATGAAGACATGGACAC; and

*MyoD*HLHb, aaaACTAGTTGCATCAGACTGTTGGTTCG.

They were then sub-cloned using the PCR-generated *Nhe*I and *Spe*I sites into a modified pCES vector in which the *lacZ*-coding region was replaced by a small fragment containing *Nhe*I and *Spe*I sites. (This vector was generated by using the primer CCGCGATATT-GAGCTAGCGTTTCAACTAGTTGGGAATTCAGCTGAGCGCC-GGTTCG along with its reverse complement.) A VP16 fragment was generated from the *Ci-Sna*VP16 construct (Fujiwara et al., 1998)

using the primers VP16f (aaaaCtaGtGCaCCaCCGACCG) and VP16b (aaaGAATTCCCTACCCACCGTACTCGTCAATTCC). This fragment was then sub-cloned onto the 3' end of the bHLH domains by using PCR-generated *Spe*I and *Eco*R1 sites.

### Gel shift assays

Binding assays were conducted as described previously (Fujiwara et al., 1998). Labeled and competitor DNAs were prepared by annealing the following oligonucleotides with their complementary fragments (bold underlined bases indicate putative T-box binding sites):

*Ci*-B, gatcCTTAA**AGGCGATAAT**GACTT

*Ci*-C, gatcTCATG**CGGCGATAAAC**GAAC

*Ci*-D, gatcACTAA**TTAGACACCT**CTAC

*Ci*-B Mut-1, gatcCTTAA**AGtCaATAAT**GACTT.

The GST-Tbx6c fusion protein was expressed using a partial *Tbx6c* cDNA (containing the full T-box DNA-binding domain) obtained from the *Ciona intestinalis* Gene Collection Release1 (Satou et al., 2002) (CiGC43g03). This coding region was fused into the pGEX-5x-1 expression vector and purified from bacterial extracts using glutathione agarose beads.

### Confocal microscopy

Transgenic embryos with GFP-expressing cells were fixed for 1 hour in 0.3% formaldehyde in seawater, mounted in Vectashield mounting medium (Vector labs, CA) and stored at -20°C. Confocal images were obtained on a Leica TCS SL1 laser scanning confocal microscope. Images were processed using the BitPlane Imaris 3.3 software package.

## Results

### Tbx6-binding sites are essential elements of the Mesp minimal enhancers

To investigate how *Mesp* expression is restricted to the emerging heart field, we isolated minimal enhancers in the 5' flanking regions of the *Ciona intestinalis* and *Ciona savignyi* *Mesp* genes (*Ci-Mesp* and *Cs-Mesp*). A 110-bp region of the *Ci-Mesp* 5' flanking sequence and a 105-bp region 5' of *Cs-Mesp* are sufficient to drive reporter gene expression in the B7.5 lineage of electroporated embryos (Fig. 1B,C,F; *Ci*-110, *Cs*-105). Short 3- to 13-bp distal deletions eliminate the activity of both enhancers (Fig. 1D-F; *Ci*-107, *Cs*-92). Comparison of these distal sequences identified a putative motif matching the consensus-binding site for *Ciona* Tbx6 transcription factors (Yagi et al., 2005). The *Ci-Mesp* distal motif is highly degenerate, matching only six of the nine base pairs comprising the Tbx6-binding consensus (including one mismatch in the core CACC; Fig. 1E). Therefore, the *Cs-Mesp* distal sequence was required to identify a putative Tbx6-binding site. There are two additional putative Tbx6-binding sites contained in each of the minimal *Mesp* enhancers (Fig. 1E). Single nucleotide changes that disrupt the distal motif abolish *Mesp-lacZ* reporter gene expression (Fig. 1F; *Ci*-B Mut-1,2, *Cs*-B Mut-1), whereas single nucleotide changes that enhance this motif have no effect (Fig. 1F; *Ci*-B Mut-T). In *Ciona intestinalis*, there is an additional putative T-box binding site (Fig. 1E, site A) upstream of the required distal motif (site B). We performed mutational analysis in the context of a longer construct that includes site A (Fig. 1F; *Ci*-138). Inclusion of the upstream T-box binding site A is sufficient for limited reporter gene expression despite the disruption of site B (Fig. 1F; *Ci*-B Mut-2 138). Mutations in the third putative T-box binding site also diminished reporter gene expression (Fig. 1F; *Ci*-C Mut-2 138).

### Tbx6c binds to the *Mesp* enhancer and participates directly in *Mesp* activation

In a comprehensive survey of *Ciona* regulatory genes, *Tbx6c* is the only T-box factor specifically expressed in the B7.5 blastomeres prior to *Mesp* activation (Imai et al., 2004). In early cleavage stages, *Tbx6c* is expressed in adjoining tail muscle blastomeres (Takatori et al., 2004) (Fig. 2A), and *Mesp-lacZ* is transiently expressed in these cells (Fig. 2B). By the 110-cell stage, *Tbx6c* expression has become restricted to the B7.5 blastomeres (Fig. 2C). At this stage, *Mesp-lacZ* staining is initiated in the B7.5 blastomeres and co-hybridization assays demonstrate the overlapping expression of *Mesp-lacZ* and *Tbx6c* (Fig. 2D). Thus, *Mesp-lacZ* reporter expression mirrors the *Tbx6c* expression pattern. Later, as gastrulation proceeds, *Tbx6c* expression expands to include the tail muscle lineages (Fig. 2E). However, *Mesp* expression (and *Mesp-lacZ* reporter expression) remains confined to the B7.5 cells as they divide (Fig. 2F) and invaginate (Fig. 2G,H).

Gel shift assays confirm specific binding of the *Tbx6c* protein to the three T-box sites contained in the minimal *Ci-Mesp* enhancer (Fig. 2I). The same single nucleotide substitutions in the distal Tbx6-binding motif that disrupt reporter gene expression also inhibit competition by unlabeled oligonucleotides (Fig. 1F, Fig. 2I; Ci-B-Mut-1). Alignment of orthologous sequences upstream of vertebrate *Mesp* genes reveals an abundance of conserved putative Tbx6-binding sites (Fig. 2J, see Discussion). Although *Tbx6c* is the best candidate for the endogenous *Mesp* activator, it is possible that the *Mesp* enhancer may also respond to the more broadly expressed *Ciona Tbx6* paralogs, *Tbx6a* or *Tbx6b*. Both genes are expressed in the B7.5 lineages, as well as in the tail muscle lineages, throughout early embryogenesis (Fig. 2H) (Takatori et al., 2004). *Tbx6c* and *Tbx6b* recognize nearly identical consensus sequences (Yagi et al., 2005). Thus, an additional activator may be required to mediate a selective response to *Tbx6c* (or to *Tbx6b* in the B7.5 blastomeres, see Discussion). Determination of the precise roles of these *Tbx6* factors in *Mesp* regulation will require further testing.

### Mesp-GFP expression visualizes heart cell migration

We employed the *Ci-Mesp* enhancer fused to GFP for visualization of embryonic heart cell migration (Fig. 3). By

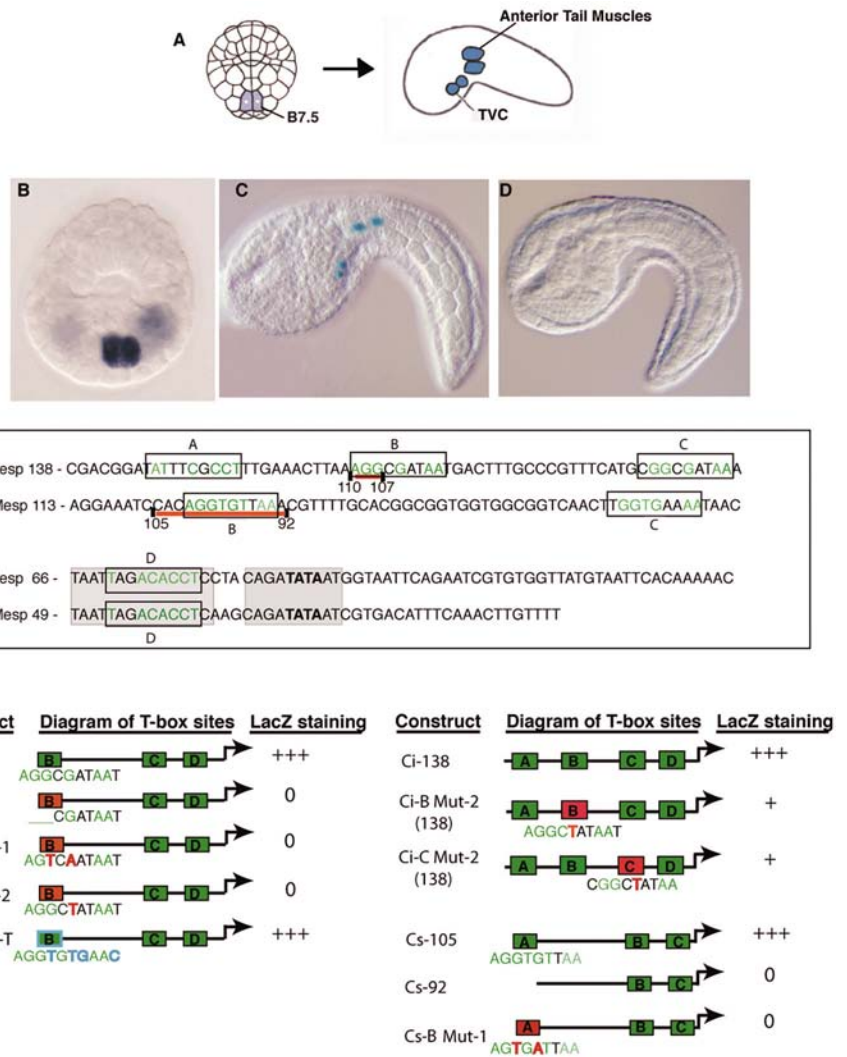


**Fig. 1.** T-box binding sites are essential components of the *Ciona Mesp* regulatory elements. (A) Diagram depicting the two lineages derived from the B7.5 cells (TVC, trunk ventral cells). (B) Transgenic, gastrulating embryo expressing the 110-bp *Ci-Mesp-lacZ* reporter gene, hybridized with a probe against *lacZ* mRNA. (C) Transgenic tailbud embryo expressing the 110-bp *Ci-Mesp-lacZ* reporter gene, stained with X-gal. (D) Transgenic tailbud embryo expressing the 107-bp *Ci-Mesp-lacZ* reporter gene, stained with X-gal. (E) Upstream sequences for *Ci-Mesp* and *Cs-Mesp*; numbers indicate the distance from the putative transcription start site. Black bars indicate minimal 110- and 105-bp enhancers. Red bars represent the distal deletions that rendered the minimal enhancers inactive. Putative T-box binding motifs are boxed and lettered; matches to the *Ciona Tbx6*-binding site are highlighted in green lettering. Gray boxed areas indicate the only stretches of conserved sequence between the two enhancers. (F) Summary of expression obtained with *Ci-Mesp-lacZ* fusion genes. Putative T-box binding motifs are indicated by lettered boxes. The motif sequences below show matches to the Tbx6 consensus-binding site (Yagi et al., 2005) in green; mutated nucleotides for disruption of the binding motif are shown in red, whereas those for enhancement of the motif are in blue. +++, strong, consistent staining of B7.5 lineages; +, weak, inconsistent staining; 0, no staining. All results are representative of at least two trials and were unambiguous for the hundreds of embryos observed in each trial.

the end of neurulation, each B7.5 blastomere has divided twice. The four descendants have a similar morphology (although the rostral TVCs are smaller) and display close membrane adhesion (Fig. 3A). During tail extension, the rostral TVCs separate from their caudal sisters, adhere to the head endoderm and migrate anteriorly along the ventral surface of this rudimentary tissue (Fig. 3B-D). Later, as the

TVCs meet along the ventral midline, they are closely apposed to the underlying epidermis and extend filopodia (see bottom inset, Fig. 3D-F). Thus, TVCs exhibit two phases of directed cell migration: anterior movements along the ventral endoderm followed by midline positioning associated with filopodial extensions.

After meeting along the midline, the TVCs initiate asymmetric cell divisions. The first round leads to a bi-linear

cluster of eight cells, four large outer cells and four small inner cells (Fig. 3G,H). After hatching, the four outer cells undergo another round of asymmetric division leading to a total of 12 cells, four larger outer cells and eight smaller inner cells (data not shown). During this same time period, the caudal B7.5 lineage differentiates into four tail muscle cells (Fig. 3H). These cells remain in their initial position, undergoing no further cell divisions or migration.

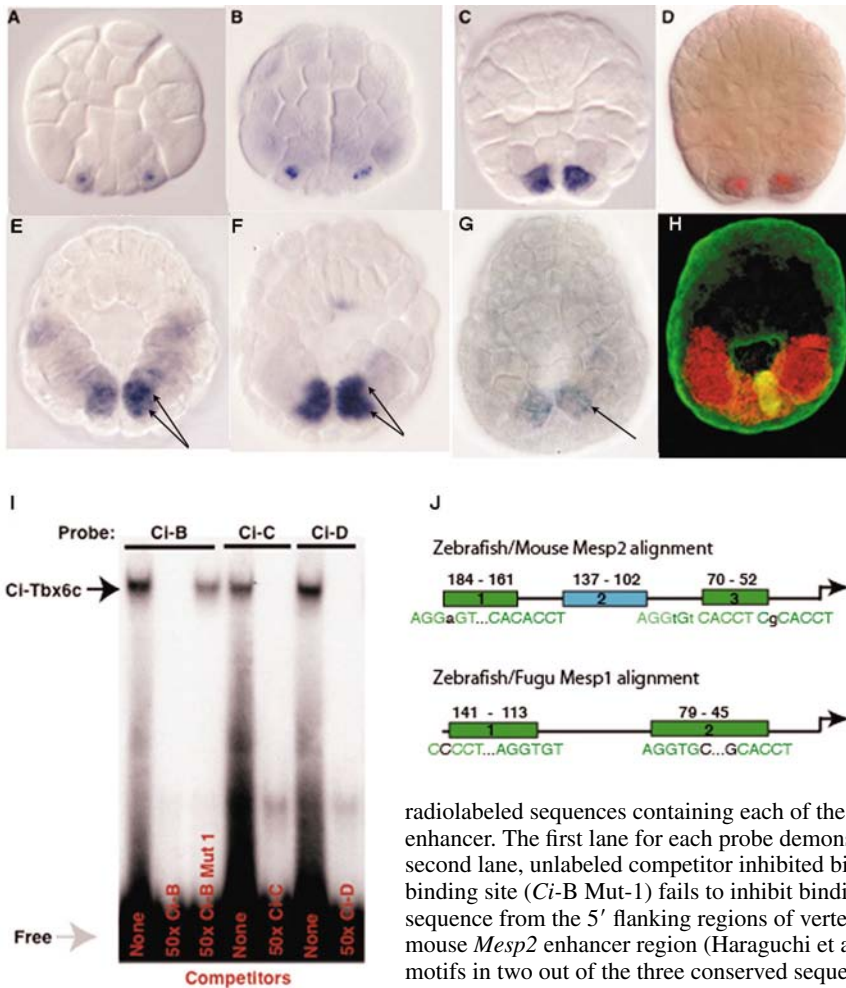


**Fig. 2.** Direct activation of *Ciona Mesp* by *Tbx6c*. (A-H) In situ hybridizations, all embryos are shown from the vegetal (future dorsal) side except for the one in G, which is shown from the ventral side; arrows in E-G indicate B7.5 lineage cells. (A) 32- to 64-cell stage embryo hybridized with a probe against *Tbx6c* (blue). (B) *Mesp-lacZ* transgenic embryo at the same stage hybridized with probe against *lacZ* (blue). (C) 110-cell embryo hybridized with probe against *Tbx6c* (blue). (D) *Mesp-lacZ* transgenic 110-cell embryo co-hybridized with probes against *Tbx6c* (blue) and *lacZ* mRNAs (red). Nuclear staining by the *lacZ* probe indicates nascent transcripts, whereas *Tbx6c* transcripts are detected in the cytoplasm owing to an earlier onset of expression. (E) Gastrulating embryo hybridized with a probe against *Tbx6c* (blue). (F) *Mesp-lacZ* transgenic embryo at the same stage hybridized with a probe against *lacZ* (blue). (G) Embryo following gastrulation hybridized with probe against *Mesp* (blue). The B7.5 lineage cells have now involuted to the ventral side, soon after this stage *Mesp* expression becomes undetectable. (H) *Mesp-lacZ* transgenic 110-cell embryo co-hybridized with probes against *Tbx6c* (red) and *lacZ* mRNA (green), such asymmetric left- or right-sided incorporation of the *Mesp-lacZ* reporter gene was a common occurrence. (I) Gel shift assays. The GST-*Tbx6c* fusion protein was incubated with

radiolabeled sequences containing each of the putative Tbx6-binding sites from the *Ci-Mesp* 110-bp enhancer. The first lane for each probe demonstrates binding to the GST-*Tbx6c* fusion protein. In the second lane, unlabeled competitor inhibited binding. For site B, a fragment containing a mutated binding site (*Ci-B* Mut-1) fails to inhibit binding (lane 3). (J) Diagrams of conserved blocks of sequence from the 5' flanking regions of vertebrate *Mesp2* and *Mesp1* genes. The characterized mouse *Mesp2* enhancer region (Haraguchi et al., 2001) is highly enriched for probable T-box binding motifs in two out of the three conserved sequence blocks. Alignment of zebrafish and *Fugu Mesp1* flanking DNA reveals a small block of conserved proximal sequence highly enriched with putative T-box binding motifs. The characterized mouse *Mesp1* enhancer region also contains numerous probable T-box binding sites (Haraguchi et al., 2001) (data not shown), but mouse and zebrafish sequences do not align. Conservation of the putative T-box binding sites is shown in green; in the motif sequence shown below, capital letters indicate conservation and green indicates a match to the consensus. Numbers indicate the distance in base pairs from the zebrafish translation start site.

**Table 1. Heart cell migration in transgenic embryos**

	n	% Normal	% Enhanced migration		% Reduced migration		% Normal migration		% Other
			+	-	+	-	+	-	
<i>Mesp-lacZ</i> or GFP	95	<b>84</b>	1.1	0	1.1	2.1	11	0	0
<i>Mesp-VP16</i>	104	7.6	3.4	0	<b>52</b>	2.5	20	0	14

Embryos were only scored if they displayed normal morphology. Embryos often displayed altered migration on one side as a result of mosaic incorporation of the transgenes, so each side of the embryo was scored independently. The 'Enhanced/Reduced migration' categories include embryos in which the majority of marked cells were found in the head/tail region, respectively. The '+/-' categories denote increased or normal number of GFP expressing cells, respectively. Each row represents the combination of two trials. For *Mesp-VP16* the 'Other' category consists of normal cell number and migration patterns, but abnormal anterior tail muscle morphology.

Numbers in bold indicate the most highly represented category for each treatment.

### Constitutively active *Mesp* drives heart differentiation in the anterior tail

A constitutively active form of *Mesp* (*Mesp-VP16*) was selectively expressed in the B7.5 lineage using the *Mesp* enhancer (Fig. 4). The VP16 moiety is a potent acidic activator (e.g. Rusch and Levine, 1997). Targeted expression of *Mesp-VP16* inhibits migration while promoting ectopic heart differentiation (Fig. 4). In tailbud embryos, the TVCs fail to separate from their caudal siblings, forming a continuous cell mass in the anterior tail region (compare Fig. 4D with 4A, see Table 1). Despite the lack of migration, transgenic cells are able to divide and differentiate as heart precursor cells (Fig. 4E-H, Tables 1, 2). When these transgenic tadpoles were reared through metamorphosis, many failed to form viable juveniles. The majority of the remaining transgenic juveniles had aberrant heart morphology (see Fig. 4G,H, Table 2). Most dramatically,

some of the *Mesp-VP16* transgenic juveniles (13%) contain ectopic beating heart tissue at the site where the tail is normally resorbed and histolyzed. Some of these juveniles had no other heart tissue (Fig. 4G, see also Movie 1 in the supplementary material). In other cases, two hearts form. Apparently, mosaic incorporation of the *Mesp-VP16* fusion gene in the caudal lineage causes the transformation of the anterior tail muscles into beating heart tissue, whereas the rostral TVCs – lacking *Mesp-VP16* – migrate to form a completely normal heart (Fig. 4H, see also Movies 2 and 3 in the supplementary material). As a control, we also expressed an activator form of the *Ciona* ortholog of *MyoD* (*MyoD-VP16*) in the B7.5 lineage. This construct did not lead to ectopic heart formation, instead it disrupted heart differentiation (see Table 2).

To further characterize the phenotype of the non-migrating cells, *Mesp-VP16* transformants were stained with lineage-

**Fig. 3.** Detailed visualization of heart cell migration. (A-H) Transgenic *Mesp-GFP* embryos. (A) Early tailbud embryo, ~12 hours post-fertilization (hpf), ventral view. (B) Tailbud embryo (~14 hpf), lateral view. (C) Ventrolateral view of a slightly more advanced embryo (~15 hpf). Note that caudal siblings are elongated with punctate accumulations of GFP. (D) Late tailbud embryo (~17 hpf), including magnified views of the two lineages. (E-G) High magnification ventral views of three sets of TVCs from progressively older embryos (~17-18 hpf). (H) Ventrolateral view of an embryo at ~18 hpf. All confocal images display GFP fluorescence in green and are shown with the anterior to the left. In A,C and H, the red channel displays phalloidin staining (Alexa-fluor 647, Molecular Probes). In B and D, the red channel displays auto-fluorescence.

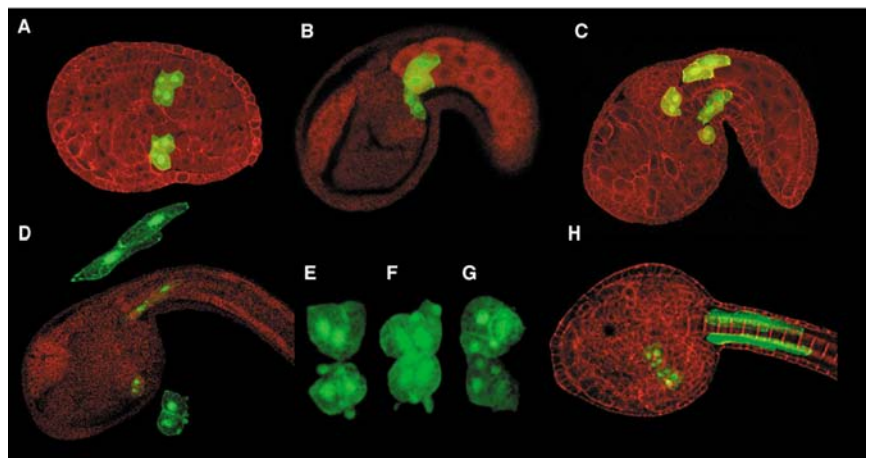


**Fig. 4.** Activator *Mesp* fusion protein blocks heart cell migration. (A-C) Transgenic *Mesp-GFP* embryos. (D-F) Embryos co-electroporated with *Mesp-VP16*. (A,D) Tailbud embryos (~14 hpf) displayed laterally. (B,E) Late tailbud embryos (~18 hpf) displayed laterally. (C,F) Late tailbud embryos (~18 hpf) displayed ventrolaterally. Embryos are oriented with anterior to the left; GFP fluorescence is in green, phalloidin staining in red. (G,H) Still shots from the movies of transgenic *Mesp-VP16* juveniles (Movies 1 and 2 in the supplementary material, respectively). Red arrowhead marks ectopic beating heart tissue; arrow marks the site of tail resorption. The site of typical heart formation is marked by a black arrowhead. E, endostyle; S, stomach. Lateral views with anterior to the left.

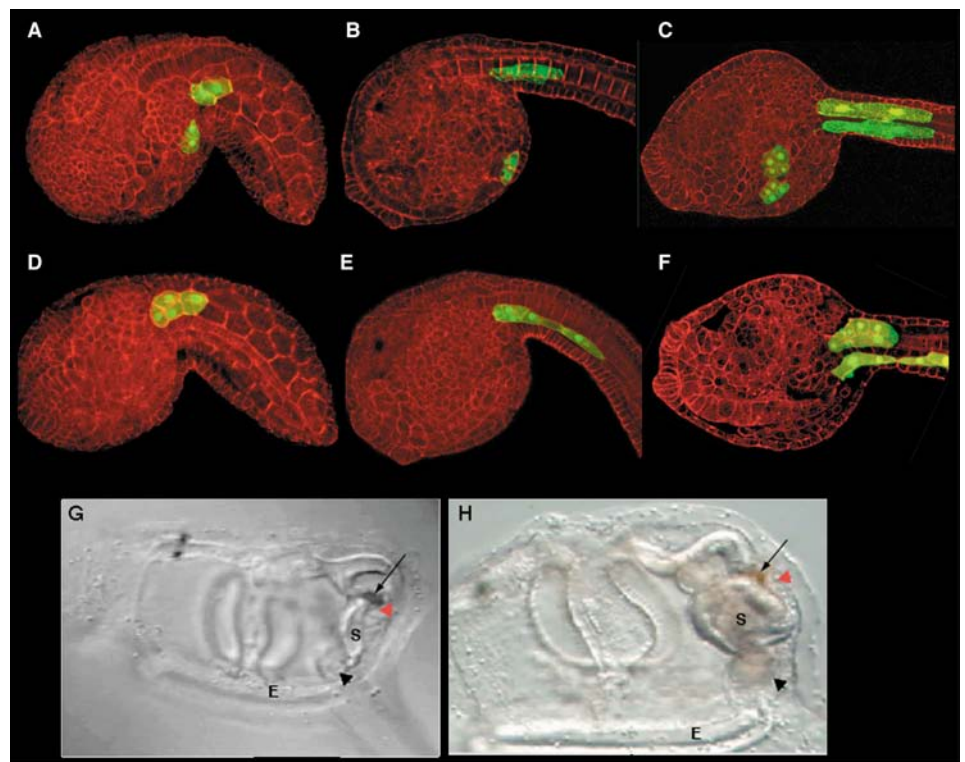


**Table 2. Transgenic juvenile heart phenotypes**

	<i>n</i>	% Normal	% Mild disruption	% Severe disruption	% No heart	% Ectopic heart
<i>Mesp-lacZ</i> or GFP	230	74	10	14	1	0
<i>Mesp-VP16</i>	120	49	2	29	9	13
<i>MyoD-VP16</i>	202	19	15	34	32	0

'Mild disruption' indicates improper beat indicative of minor myocardial abnormalities. 'Severe disruption' generally indicates major to nearly complete loss of beating myocardial tissue. The 'No heart' category includes some juveniles in which a pericardial chamber was present but no beating myocardial tissue was observed.

Data for the *Mesp-VP16* and *MyoD-VP16* juveniles represent two trials, whereas the *Mesp-lacZ/GFP* control data is from four trials. Many of the transgenic *Mesp-VP16* juveniles died soon after metamorphosis or displayed general morphological disruptions. This may be due to the loss of *Raldh* expression (and the subsequent interference with retinoic acid synthesis) in fully penetrant *Mesp-VP16* juveniles (see Table 3).

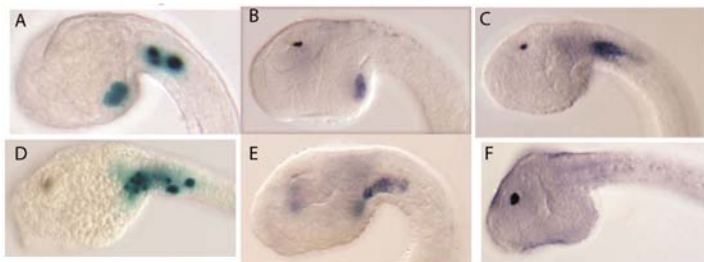


**Fig. 5.** Activator and repressor *Mesp* fusion proteins alter the expression of B7.5 lineage markers. (A-C) Control. (D-F) *Mesp-VP16*. (A,D) Transgenic *Mesp-lacZ* embryos. (B,E) Embryos stained using a probe for *Hand-like*. (C,F) Embryos stained using a probe for *Raldh2*. All embryos are shown laterally, anterior to the left.

specific marker genes (Fig. 5). The two B7.5 lineages can be distinguished by the expression of *Hand-like* (*Ci-Notr1c*) in the TVCs, and retinaldehyde dehydrogenase 2 (*Ci-Raldh2*) in the anterior tail muscles (Fig. 5B,C) (Nagatomo and Fujiwara, 2003; Satou et al., 2004). Transgenic *Mesp-VP16* embryos display *Hand-like* expression in the non-migrating cluster of B7.5 lineage cells (Fig. 5E), whereas *Raldh2* expression was reduced or eliminated (Fig. 5F). These observations suggest that *Mesp-VP16* causes the transformation of the caudal B7.5 lineage, so that these cells differentiate into heart cells rather than anterior tail muscles.

## Discussion

### Tbx6-Mesp interactions during chordate heart development

The detailed characterization of *Mesp* enhancers in *Ciona*

**Fig. 6.** Model for heart specification in *Ciona*. Stages are shown on the top line. (A) At the 16- to 64-cell stages maternal Macho 1 directs the expression of *Tbx6b* and *Tbx6c*, whereas maternal  $\beta$ -catenin directs the expression of an additional activator. At the 110-cell stage, Tbx6 and 'Activator X' drive the expression of *Mesp* in the B7.5 cells. *Mesp* expression initiates conditional heart specification (represented by the red and yellow pattern). During gastrulation, the B7.5 cells have divided to form a cluster of four cells. An inductive 'Signal X' then synergizes with *Mesp* to permit further heart differentiation in the anterior daughters, whereas the posterior daughters revert to an anterior tail muscle fate. (B) Targeted expression of the constitutively active MespVP16 bypasses the requirement for the inductive signal, leading to heart differentiation in the entire B7.5 lineage.

*intestinalis* and *Ciona savignyi* led to the identification of *Tbx6* as a crucial activator of the emerging cardiac field. Because of their degeneracy, it was not possible to identify *Tbx6* sites through the use of phylogenetic footprinting or clustering of binding motifs. Instead, identification depended on the combination of functional assays and a comparison of orthologous regulatory elements from the two *Ciona* species. The ability of transcription factors to bind degenerate sites is an important caveat when attempting to identify regulatory elements using computational methods.

*Tbx6c* is probably necessary, but not sufficient, for the activation of *Mesp* in the B7.5 lineage. *Mesp* expression relies on two maternal factors, Macho 1 and  $\beta$ -catenin (Satou et al., 2004) (Fig. 6A). Macho 1 is upstream of both *Tbx6b* and *Tbx6c*, and thus presumably regulates *Mesp* expression through these genes. By contrast,  $\beta$ -catenin is likely to direct *Mesp* expression through a *Tbx6*-independent pathway. It is conceivable that BMP signaling works in concert with *Tbx6c* to activate *Mesp*, as point mutations in a putative SMAD-binding site nearly abolished the activity of an otherwise normal *Mesp-lacZ* fusion gene (B.D., unpublished). A second activator would also explain the restriction of *Mesp* to the B7.5 lineage during gastrulation, despite expansion of the *Tbx6c* expression pattern into the developing tail muscles (see Fig. 2E). In principle, a localized repressor could delimit *Mesp* expression; however, extensive mutagenesis and internal deletions within the *Mesp* minimal enhancer did not cause expansion of the reporter gene expression (data not shown).

*Tbx6-Mesp* interactions in *Ciona* raise the possibility that Tbx6 activated *Mesp* in the ancestral chordates. Vertebrates contain two closely linked *Mesp* paralogs, one primarily involved in heart development (*Mesp1*) and the other in

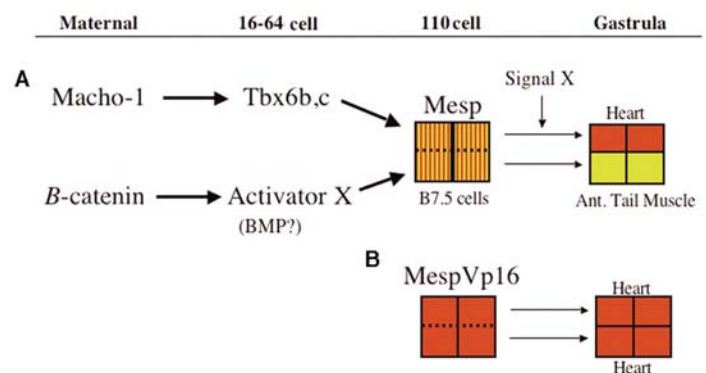


**Table 3. Marker gene expression in transgenic embryos**

	<i>n</i>	% Normal	% Reduced	% No stain	% Ectopic
Control-Raldh	40	83	15	2.5	0
<i>Mesp</i> -VP16-Raldh	33	36	42	15	6
Control-Hand-like	161	94	1.2	0	4.3
<i>Mesp</i> -VP16-Hand-like	71	39	0	0	61

Embryos were only scored if they displayed normal morphology, scoring refers to staining pattern. 'Reduced' indicates very low levels of staining in comparison with controls (for example, see Fig. 5F). For *Raldh*, 'Ectopic' indicates staining in the head region, this staining was always very weak. For *Hand-like*, 'Ectopic' indicates staining in or near the tail region (see Fig. 5E).

somitogenesis (*Mesp2*) (Kitajima et al., 2000; Takahashi et al., 2005). There are indications that both vertebrate *Mesp* genes maintain the ancestral requirement for Tbx6 activation. Alignment of vertebrate *Mesp1* and *Mesp2* 5' flanking sequences identify numerous potential T-box binding motifs (Fig. 2F). Moreover, the *Tbx6* and *Mesp1* expression domains overlap in the early primitive streak of mice (Chapman et al., 1996; Saga et al., 1996), and *Mesp2* expression is lost in *Tbx6*<sup>-</sup>/*Tbx6*<sup>-</sup> mutant mice (White et al., 2003). It is conceivable that the ancestral gene was also regulated by Notch signaling. *Mesp2* is one of the first read-outs of the periodic expression of Notch signaling genes (the somitogenic clock). In chick, the somitogenesis clock is active in the emerging heart field at the time when *Mesp1* may be activated (Jouve et al., 2002). The *Ciona Mesp* minimal enhancers lack obvious Su(H)-binding sites. However, preliminary studies suggest that the inhibition of Notch signaling diminishes *Mesp* expression (B.D., unpublished). Further studies will be required to determine whether Tbx6 and Notch regulate *Mesp* in the heart field of *Ciona* and vertebrates.

### Constitutively active *Mesp* uncouples heart cell specification and migration

The detailed analysis of *Mesp*-GFP reporter expression in early *Ciona* embryos provided single-cell resolution of the directed migration of heart progenitors. Confocal imaging identified two phases in the directed movement of heart cells: anterior migration and ventral fusion. Intriguingly, a comparable, possibly conserved, bi-phasic mode of heart cell migration has recently been characterized in zebrafish (Nathalia Glickman, personal communication). The simplicity of *Ciona* cell lineages, and the ability to independently manipulate cardiac migration and specification programs (see below), should permit the systematic identification of the signals and networks underlying the early migration of heart cells.

Previous studies of *Mesp* function have been interpreted as indicating primary roles in either heart cell migration (Kitajima et al., 2000) or specification (Satou et al., 2004). In mice, chimeric *Mesp1/Mesp2* knockout cells fail to migrate into the forming heart, but this might be secondary to a disruption of early specification events. In *Ciona*, *Mesp* morpholinos block the expression of heart markers, but this might be secondary to a disruption of early migration. The present study indicates that the primary function of *Mesp* is cardiac specification. The demonstration that an activator form of *Mesp* can drive the differentiation of ectopic beating heart tissue suggests that *Mesp* acts as a cardiac determinant independently of any role

in migration. The manipulation of *Mesp* function led to the uncoupling of heart cell migration and specification. It is not clear why the activator form of *Mesp* interferes with migration. However, *Mesp* is transiently expressed in the B7.5 lineage, and is lost from the heart progenitors prior to the onset of migration. Perhaps this downregulation is essential for migration and the prolonged expression of *Mesp-VP16* blocks migration. Regardless of the mechanism, the uncoupling of heart cell migration and specification sets the stage for the detailed investigation of each process.

### Determination of the heart field within the *Mesp* expression domain

In both vertebrates and *Ciona*, the *Mesp* expression domain extends beyond the definitive heart field into neighboring mesodermal precursor populations. Thus, *Mesp* expression alone is not sufficient to drive cardiac specification. Preliminary studies indicate that an inductive event determines the definitive heart field within the *Mesp* expression domain (B.D., unpublished). According to our current model (Fig. 6A), *Mesp* specifies a field of potential heart cells. Subsequently, inductive signals release this latent cardiac potential in a subset of the *Mesp* expression domain. This model is consistent with the ability of a constitutively active form of *Mesp* to drive heart specification in the entire *Mesp* expression domain, bypassing the inductive signal (Fig. 6B). This model is also consistent with recent findings regarding the broad cardiac potential of the early chick mesoderm (Eisenberg and Eisenberg, 2004).

A role for *Mesp* in heart development may have first evolved in the chordates. Despite conservation of the core cardiac gene network (*Nkx2.5-Gata4-Hand*) in *Drosophila* and vertebrates (Zaffran and Frasch, 2002), there is no ortholog of *Mesp* expressed in the *Drosophila* heart field (Moore et al., 2000). In both mice and *Ciona*, *Mesp* is expressed in the emerging cardiac mesoderm prior to the initial expression of the core heart transcription factors (Saga et al., 2000; Satou et al., 2004). Thus it appears that *Mesp* was recruited during chordate evolution to act upstream of these conserved regulatory genes in setting up the initial heart field. Identification of *Mesp* downstream targets in *Ciona* will clarify the link between *Mesp* and the established heart gene network.

We thank David Keys and Li Weng for their assistance in initially identifying the *Mesp* enhancer; Nori Satoh and Yutaka Satou for generously providing us with both *Ciona intestinalis* Gene Collections; and Kasumi Yagi and Lionel Christiaen for their comments and insights. This work was supported by National Institutes of Health Grant HD037105 and National Science Foundation Grant IOB-0445470 (to M.L.). B.D. is supported by an NRSA fellowship (F32 GM069225).

### Supplementary material

Supplementary material for this article is available at <http://dev.biologists.org/cgi/content/full/132/21/4811/DC1>

### References

- Chapman, D. L., Agulnik, I., Hancock, S., Silver, L. M. and Papaioannou, V. E. (1996). Tbx6, a mouse T-Box gene implicated in paraxial mesoderm formation at gastrulation. *Dev. Biol.* **180**, 534-542.
- Corbo, J. C., Levine, M. and Zeller, R. W. (1997). Characterization of a notochord-specific enhancer from the Brachyury promoter region of the ascidian, *Ciona intestinalis*. *Development* **124**, 589-602.



- Davidson, B. and Levine, M.** (2003). Evolutionary origins of the vertebrate heart: Specification of the cardiac lineage in *Ciona intestinalis*. *Proc. Natl. Acad. Sci. USA* **100**, 11469-11473.
- Eisenberg, L. M. and Eisenberg, C. A.** (2004). An in vitro analysis of myocardial potential indicates that phenotypic plasticity is an innate property of early embryonic tissue. *Stem Cells Dev.* **13**, 614-624.
- Fujiwara, S., Corbo, J. C. and Levine, M.** (1998). The snail repressor establishes a muscle/notochord boundary in the *Ciona* embryo. *Development* **125**, 2511-2520.
- Harafuji, N., Keys, D. N. and Levine, M.** (2002). Genome-wide identification of tissue-specific enhancers in the *Ciona* tadpole. *Proc. Natl. Acad. Sci. USA* **99**, 6802-6805.
- Haraguchi, S., Kitajima, S., Takagi, A., Takeda, H., Inoue, T. and Saga, Y.** (2001). Transcriptional regulation of *Mesp1* and *Mesp2* genes: differential usage of enhancers during development. *Mech. Dev.* **108**, 59-69.
- Hirano, T. and Nishida, H.** (1997). Developmental fates of larval tissues after metamorphosis in ascidian *Halocynthia roretzi*. I. Origin of mesodermal tissues of the juvenile. *Dev. Biol.* **192**, 199-210.
- Imai, K. S., Hino, K., Yagi, K., Satoh, N. and Satou, Y.** (2004). Gene expression profiles of transcription factors and signaling molecules in the ascidian embryo: towards a comprehensive understanding of gene networks. *Development* **131**, 4047-4058.
- Jouve, C., Imura, T. and Pourquie, O.** (2002). Onset of the segmentation clock in the chick embryo: evidence for oscillations in the somite precursors in the primitive streak. *Development* **129**, 1107-1117.
- Kitajima, S., Takagi, A., Inoue, T. and Saga, Y.** (2000). *Mesp1* and *Mesp2* are essential for the development of cardiac mesoderm. *Development* **127**, 3215-3226.
- MacLean, D. W., Meedel, T. H. and Hastings, K. E.** (1997). Tissue-specific alternative splicing of ascidian troponin I isoforms. Redesign of a protein isoform-generating mechanism during chordate evolution. *J. Biol. Chem.* **272**, 32115-32120.
- Meedel, T. H., Farmer, S. C. and Lee, J. J.** (1997). The single MyoD family gene of *Ciona intestinalis* encodes two differentially expressed proteins: implications for the evolution of chordate muscle gene regulation. *Development* **124**, 1711-1721.
- Moore, A. W., Barbel, S., Jan, L. Y. and Jan, Y. N.** (2000). A genome wide survey of basic helix-loop-helix factors in *Drosophila*. *Proc. Natl. Acad. Sci. USA* **97**, 10436-10441.
- Nagatomo, K. and Fujiwara, S.** (2003). Expression of *Raldh2*, *Cyp26* and *Hox-1* in normal and retinoic acid-treated *Ciona intestinalis* embryos. *Gene Expr. Patterns* **3**, 273-277.
- Rusch, J. and Levine, M.** (1997). Regulation of a *dpp* target gene in the *Drosophila* embryo. *Development* **124**, 303-311.
- Saga, Y., Hata, N., Kobayashi, S., Magnuson, T., Seldin, M. F. and Taketo, M. M.** (1996). *Mesp1*: a novel basic helix-loop-helix protein expressed in the nascent mesodermal cells during mouse gastrulation. *Development* **122**, 2769-2778.
- Saga, Y., Kitajima, S. and Miyagawa-Tomita, S.** (2000). *Mesp1* expression is the earliest sign of cardiovascular development. *Trends Cardiovasc. Med.* **10**, 345-352.
- Satou, Y., Yamada, L., Mochizuki, Y., Takatori, N., Kawashima, T., Sasaki, A., Hamaguchi, M., Awazu, S., Yagi, K., Sasakura, Y. et al.** (2002). A cDNA resource from the basal chordate *Ciona intestinalis*. *Genesis* **33**, 153-154.
- Satou, Y., Imai, K. S. and Satoh, N.** (2004). The ascidian *Mesp* gene specifies heart precursor cells. *Development* **131**, 2533-2541.
- Takahashi, Y., Kitajima, S., Inoue, T., Kanno, J. and Saga, Y.** (2005). Differential contributions of *Mesp1* and *Mesp2* to the epithelialization and rostro-caudal patterning of somites. *Development* **132**, 787-796.
- Takatori, N., Hotta, K., Mochizuki, Y., Satoh, G., Mitani, Y., Satoh, N., Satou, Y. and Takahashi, H.** (2004). T-box genes in the ascidian *Ciona intestinalis*: characterization of cDNAs and spatial expression. *Dev. Dyn.* **230**, 743-753.
- White, P. H., Farkas, D. R., McFadden, E. E. and Chapman, D. L.** (2003). Defective somite patterning in mouse embryos with reduced levels of *Tbx6*. *Development* **130**, 1681-1690.
- Yagi, K., Takatori, N., Satou, Y. and Satoh, N.** (2005). *Ci-Tbx6b* and *Ci-Tbx6c* are key mediators of the maternal effect gene *Ci-macho1* in muscle cell differentiation in *Ciona intestinalis* embryos. *Dev. Biol.* **282**, 535-549.
- Zaffran, S. and Frasch, M.** (2002). Early signals in cardiac development. *Circ. Res.* **91**, 457-469.